Brief Report

Beam hardening artifact reduction using dual energy computed tomography: implications for myocardial perfusion studies

Gaston A. Rodriguez-Granillo[1], Patricia Carrascosa[1], Silvina Cipriano[1], Macarena De Zan[1], Alejandro Deviggiano[1], Carlos Capunay[1], Ricardo C. Cury[2]

[1]Department of Cardiovascular Imaging, Diagnóstico Maipú, Buenos Aires, Argentina; [2]Miami Cardiac and Vascular Institute and Baptist Health of South Florida, Miami, FL, USA

Correspondence to: Gaston A. Rodriguez-Granillo, MD, PhD. Av Maipú 1668, Vicente López (B1602ABQ), Buenos Aires, Argentina. Email: grodriguezgranillo@gmail.com.

Background: Myocardial computed tomography perfusion (CTP) using conventional single energy (SE) imaging is influenced by the presence of beam hardening artifacts (BHA), occasionally resembling perfusion defects and commonly observed at the left ventricular posterobasal wall (PB). We therefore sought to explore the ability of dual energy (DE) CTP to attenuate the presence of BHA.

Methods: Consecutive patients without history of coronary artery disease who were referred for computed tomography coronary angiography (CTCA) due to atypical chest pain and a normal stress-rest SPECT and had absence or mild coronary atherosclerosis constituted the study population. The study group was acquired using DE and the control group using SE imaging.

Results: Demographical characteristics were similar between groups, as well as the heart rate and the effective radiation dose. Myocardial signal density (SD) levels were evaluated in 280 basal segments among the DE group (140 PB segments for each energy level from 40 to 100 keV; and 140 reference segments), and in 40 basal segments (at the same locations) among the SE group. Among the DE group, myocardial SD levels and myocardial SD ratio evaluated at the reference segment were higher at low energy levels, with significantly lower SD levels at increasing energy levels. Myocardial signal-to-noise ratio was not significantly influenced by the energy level applied, although 70 keV was identified as the energy level with the best overall signal-to-noise ratio. Significant differences were identified between the PB segment and the reference segment among the lower energy levels, whereas at ≥70 keV myocardial SD levels were similar. Compared to DE reconstructions at the best energy level (70 keV), SE acquisitions showed no significant differences overall regarding myocardial SD levels among the reference segments.

Conclusions: BHA that influence the assessment of myocardial perfusion can be attenuated using DE at 70 keV or higher.

Keywords: Myocardial perfusion; perfusion defect; myocardial infarction; ischemia; cardiac; computed tomography (CT)

Submitted Dec 29, 2014. Accepted for publication Jan 23, 2015.
doi: 10.3978/j.issn.2223-3652.2015.01.13
View this article at: http://dx.doi.org/10.3978/j.issn.2223-3652.2015.01.13

Introduction

During the past decade, the poor relationship between the degree of stenosis and the presence of ischemia has driven the need to assess the physiological impact of a given atherosclerotic lesion, particularly of moderate lesions (1,2). Myocardial perfusion imaging by means of computed tomography (CT) shows promise to provide an incremental diagnostic and prognostic value over computed tomography coronary angiography (CTCA) (3-6). Nevertheless, the assessment of myocardial perfusion using conventional single energy (SE) acquisitions is influenced by the presence of beam hardening artifacts (BHA) (7,8). These artifacts

are related to the polychromatic nature of X-rays and to the energy-dependency of X-ray attenuation, and lead to a significant drop in attenuation levels in areas adjacent to highly enhanced structures, commonly resembling perfusion defects in certain left ventricular segments during CTCA (8). Dual energy (DE) CT imaging has the potential to attenuate or even elucidate some of these technical issues observed in SE imaging, mainly driven by its ability to obtain synthesized monochromatic image reconstructions (7,9). We therefore sought to explore the ability of DE CTP to mitigate the presence of BHA in a non-diabetic population with normal myocardial perfusion and without evidence of coronary artery disease (CAD).

Methods

The present was a single-center, investigator-driven, observational study, that involved consecutive patients without a history of CAD who were referred for CTCA evaluation at our institution due to atypical chest pain and evidence of a normal stress-rest single-photon emission computed tomography (SPECT) within the previous 3 months. All patients included were >18 years old, in sinus rhythm, able to maintain a breath-hold for ≥15 seconds, without a history of contrast related allergy, renal failure, or haemodynamic instability. Additional exclusion criteria comprised a body mass index >32 kg/m^2, a history of previous myocardial infarction, percutaneous or surgical coronary revascularization, severe valve disease, chronic heart failure, chronic obstructive pulmonary disease, or high degree atrioventricular block. Patients with diabetes, left ventricular hypertrophy, and with obstructive (≥50% stenosis) atherosclerotic coronary lesions were also excluded. In addition, patients with intrascan mild heart rhythm abnormalities leading to motion artifacts such as premature beats and heart rate <40 bpm were excluded. Two cohorts of patients were sequentially included. The study group was acquired using DE acquisition, and the control group using conventional SE scan.

Image acquisition

Patients with a heart rate of more than 65 bpm received 50 mg metoprolol orally or 5 mg intravenous propralonol if needed in order to achieve a target heart rate of less than 60 bpm.

Patients were scanned using a DE scanner equipped with gemstone detectors with fast primary speed and low afterglow designed for spectral imaging (Discovery HD 750, GE Medical Systems, Milwaukee, USA). All scans were performed using prospective ECG gating, using a 100 msec padding centered at 75% of the cardiac cycle. Other scanner-related parameters were a collimation width of 0.625 mm and a slice interval of 0.625 mm. Maximum tube voltage and current of SE scans were adjusted according to the body habitus (100 kV or 120 kV for patients with body mass index <30 kg/m^2 or larger, respectively). DE imaging was performed by rapid switching (0.3-0.5 milliseconds) between low and high tube potentials (80-140 kV) from a single source, thereby allowing the reconstruction of low and high energy projections and generation of monochromatic image reconstructions with 10 keV increments from 40 to 140 keV. Iterative reconstruction was performed in all cases at 40% ASIR (Adaptive Statistical Iterative Reconstruction). For DE acquisitions, 60 keV is so far the lowest monoenergetic level available for the reconstruction of images utilizing an iterative reconstruction algorithm. A dual phase protocol with 50-70 mL of iodinated contrast (iobitridol, Xenetix 350^{TM}, Guerbet, France), followed by a 30-40-mL saline flush was injected through an arm vein. A bolus tracking technique was used to synchronize the arrival of contrast at the level of the coronary arteries with the start of the scan. Image acquisition was performed after sublingual administration of 2.5-5 mg of isosorbide dinitrate.

The institution's Ethics Committee approved the study protocol, which complied with the Declaration of Helsinki, and written informed consent was obtained from all patients.

Signal density (SD) levels at the posterobasal segment

CTCA image analysis was performed off-line on a dedicated workstation, using a commercially available dedicated software tool (AW 4.6, GE Healthcare). Two experienced observers (GRG, PC) were randomly assigned to independently analyze patients of either of the two groups. CT images were analyzed at mid diastole using a smooth filter in axial planes and multiplanar reconstructions. Short axis views were obtained initially using 5 mm average multiplanar reconstructions, with the full dataset available for the reader. A basal short axis plane including the mitral valve and the left ventricular outflow tract was obtained in order to evaluate myocardial SD and noise (standard deviation of myocardial SD) at two independent 20 mm^2 regions of interest: (I) the left ventricular posterobasal wall

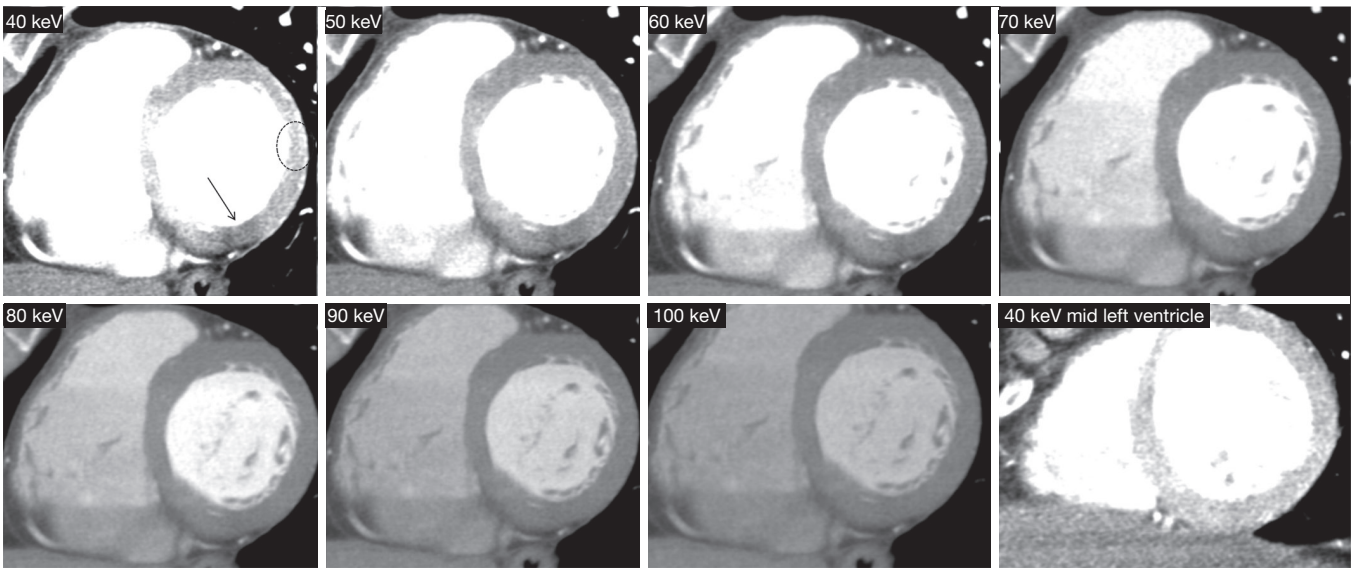

Figure 1 Basal short axis view at the left ventricular outflow tract using dual energy imaging at increasing energy levels from 40 to 100 keV. The posterobasal wall segment (arrow) depicts a significant drop in myocardial signal density at the lowest energy levels (arrow) with normal attenuation at the reference segment (dotted circle), whereas at mid and higher energy levels (≥70 keV) the myocardial signal density is homogeneous. The bottom right panel depicts the mid left ventricular wall at 40 keV, showing no beam hardening artifacts.

(PB), an inferolateral segment not included in the AHA 17-segment model that is commonly affected by BHA; (II) the anterolateral segment as a reference (*Figures 1,2*) (8). Left ventricular and right ventricular chamber mean SD were evaluated at basal, mid and apical short axis.

Measurements among the DE group were performed at different energy levels ranging from 40 to 100 keV, with 10 keV increments. SD ratio, which is highly related to myocardial blood flow measured by microspheres, was determined as previously described: myocardial SD/left ventricular blood pool SD (10). Myocardial SD, SD ratio, and signal-to-noise ratio were evaluated.

CT effective radiation dose was derived by multiplying the dose-length product with the weighting (k) value of 0.014 mSv/mGy/cm for chest examinations, as suggested by the Society of Cardiovascular Computed Tomography (11).

Statistical analysis

Discrete variables are presented as counts and percentages, and continuous variables as mean ± standard deviation. Comparisons among groups were performed using paired samples *t*-test, independent samples *t*-test, analysis of variance (ANOVA), chi square tests, or Fisher's exact tests, as indicated. Post-hoc comparisons were explored using least significant difference (LSD) tests. We explored correlations between the posterobasal wall SD and variables thought to be related to the presence BHA using Spearman correlation coefficients. A two-sided p value of less than 0.05 indicated statistical significance. Statistical analyses were performed with use of SPSS software, version 22 (Chicago, Illinois, USA).

Results

Forty patients constituted the study population (DE group, n=20; SE group, n=20). The mean age was 59.6±12.0 years, and 28 (70%) were male. Demographical characteristics were similar between groups, as well as the heart rate and the effective radiation dose (*Table 1*).

Myocardial SD levels were evaluated in 280 basal segments among the DE group (140 PB segments for each energy level from 40 to 100 keV; and 140 reference segments), and in 40 basal segments (20 PB and 20 reference segments) among the SE group.

Myocardial SD levels using DE and SE imaging

Among the DE group, myocardial SD levels and myocardial SD ratio at the reference segment were higher at low energy

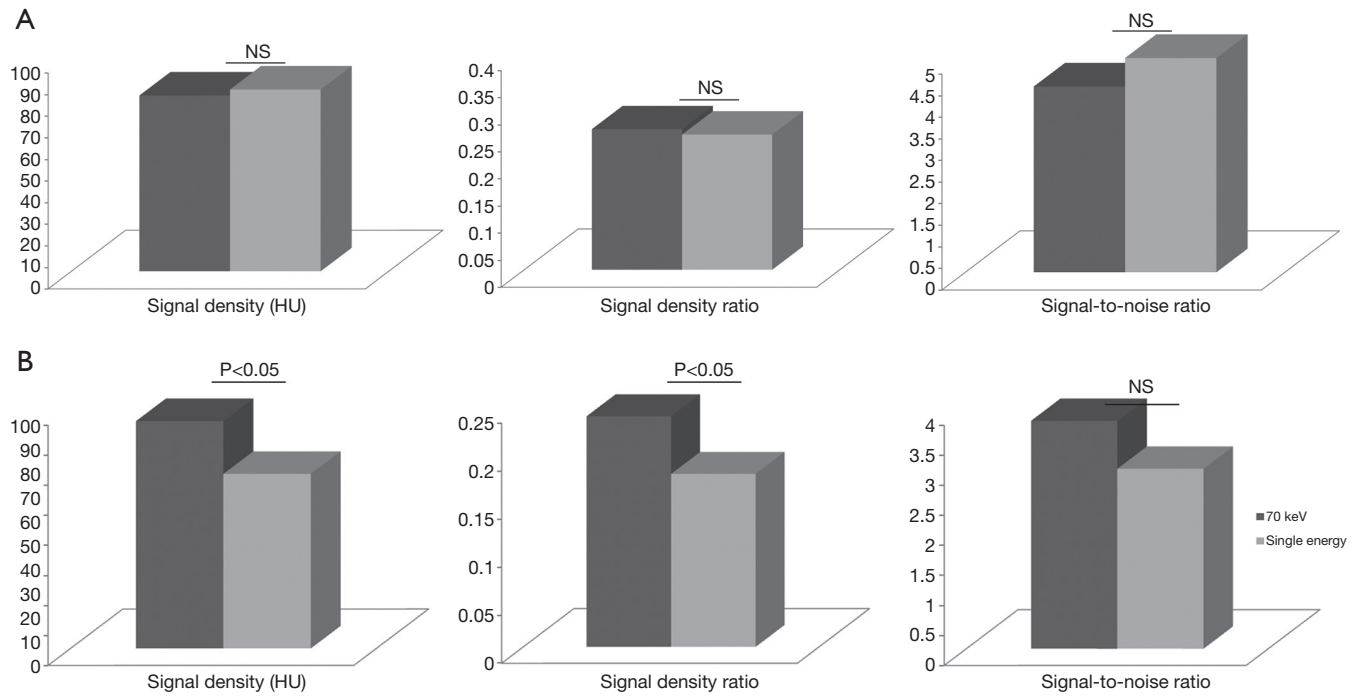

Figure 2 Myocardial signal density, signal density ratio (defined as myocardial signal density/left ventricular chamber signal density), and signal-to-noise ratio at the reference segment (A) and at the posterobasal segment (B) using single energy and dual energy imaging at 70 keV. No significant differences are observed between groups at the reference segments (A) whereas among the PB segments (B) SE acquisitions showed significantly lower signal density, signal density ratio, and signal-to-noise ratio levels; although these differences reached statistical significance only for the first two.

Table 1 Demographical characteristics

Characteristics	Dual energy, (n=20)	Single energy, (n=20)	P
Age (years)	60.8±9.9	58.5±14.3	0.56
Male (n, %)	12, 60%	16, 80%	0.30
Hypertension (n, %)	12, 60%	10, 50%	0.75
Hypercholesterolemia (n, %)	11, 55%	10, 50%	0.99
Smoking (n, %)	7, 35%	2, 10%	0.13
Heart rate (bpm ± SD)	63.3±5.8	63.1±5.4	0.93
Effective dose (mSv ± SD)	3.1±0.4	3.3±0.7	0.34

Comparisons performed using Fisher's exact test.

levels, with significantly lower SD levels at increasing energy levels (*Table 2* and *Figure 1*). In turn, myocardial signal-to-noise ratio was not significantly influenced by the energy level applied, although 70 keV was identified as the energy level with the best overall signal-to-noise ratio (*Table 2*).

DE imaging at the reference segment of the best energy level (70 keV, based on the highest signal-to-noise levels) showed similar SD, SD ratio, and signal-to-noise ratio levels compared to SE acquisitions (*Figure 2A*). In turn, among the PB segments (*Figure 2B*) SE acquisitions showed overall significantly lower SD, SD ratio, and signal-to-noise ratio levels; although these differences reached statistical significance only for the first two (*Figure 2B*).

Significant paired differences were found between the PB segment and the reference segment among the lowest energy levels, whereas at ≥70 keV myocardial SD levels were

Table 2 Differences between the PB and reference segments regarding myocardial signal density, signal density ratio, and signal-to-noise ratio among different energy levels using dual energy acquisitions

Differences	40 keV	50 keV	60 keV	70 keV	80 keV	90 keV	100 keV	P (ANOVA)
Myocardial signal density								
PB	178.2±76.2*	127.7±47.0*	95.7±31.0	75.8±21.5	63.8±15.4	55.9±13.5	49.9±11.6*	<0.0001
Reference	222.9±56.5*	152.5±37.0*	108.6±26.1*	81.4±19.8	63.8±16.1	52.8±14.4*	45.1±13.5*	<0.0001
P value	0.005	0.008	0.02	0.13	1.0	0.31	0.09	
Myocardial signal density ratio								
PB	0.19±0.09	0.21±0.09	0.22±0.09	0.24±0.1	0.27±0.1	0.30±0.1	0.33±0.1*	<0.0001
Reference	0.24±0.09	0.24±0.09	0.25±0.1	0.26±0.1	0.27±0.1	0.28±0.1	0.30±0.1	0.66
P value	0.003	0.005	0.02	0.14	0.99	0.38	0.12	
Myocardial signal-to-noise ratio								
PB	2.8±1.3*	2.9±1.3*	3.4±1.4	3.8±1.5	3.8±1.2	3.4±1.2	3.3±1.2	0.17
Reference	3.7±1.8	3.7±1.3	4.1±1.4	4.3±1.5	4.0±1.5	3.3±1.2*	3.2±1.4*	0.11
P value	0.007	0.021	0.02	0.09	0.35	0.85	0.48	

*P<0.05 *vs*. 70 keV (post-hoc comparisons using LSD tests). Abbreviations: PB, posterobasal; ANOVA, analysis of variance; LSD, least significant difference.

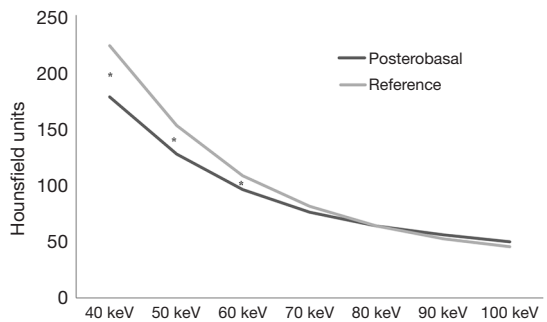

Figure 3 Pairwise comparisons between myocardial signal density levels at the same basal short axis plane (posterobasal wall versus reference segment). Significant differences (*denotes P<0.05) are present between the posterobasal segment and a reference segment among the lowest energy levels (40-60 keV), whereas at ≥70 keV signal density levels are similar.

similar (*Figure 3*). Within the SE group, we did not identify significant correlations between PB SD levels and body mass index (P=0.68), heart rate (P=0.35), basal left ventricular chamber SD (P=0.67), right ventricular chamber SD (P=0.29), or descending aorta SD (P=0.69). Likewise, within the DE group, we did not identify significant relationships between posterobasal SD levels and body mass index at any energy level (40 keV; r=−0.36, P=0.13). However, a significant relationship was found between posterobasal SD levels and descending aorta SD until 70 keV (r=0.48, P=0.04), whereas at higher levels no relationship was found (80 keV; r=0.33, P=0.17; 90 keV; r=0.30, P=0.22; 100 keV; r=0.36, P=0.12). On the other hand posterobasal SD levels at energy levels ≥70 keV were not significantly related to heart rate (70 keV; r=0.07, P=0.79), basal left ventricular chamber SD (70 keV; r=0.41, P=0.08), or right ventricular chamber SD (70 keV; r=0.27, P=0.26).

Discussion

The main finding of the present study was that in a non-diabetic population with normal myocardial perfusion and without evidence of CAD, BHA were attenuated using DE imaging.

Numerous studies have demonstrated the ability of cardiac computed tomography to assess myocardial perfusion (CTP) in diverse clinical scenarios (12,13). CTP can be evaluated using two approaches; static CTP, and dynamic CTP. Static CTP, as the one used in our study, enables a qualitative assessment of CT attenuation-based myocardial perfusion assessment founded on myocardial attenuation (signal density, SD) levels, as well as the measurement of myocardial SD levels. On the other hand, dynamic CTP allows a quantitative estimate of myocardial time-attenuation curves and other parameters such as myocardial blood flow. Even though both approaches have a good agreement and similar diagnostic performance,

dynamic CTP is related to significantly higher radiation exposure compared to static CTP (14,15).

BHA is deemed an important shortcoming of CTP techniques (16). These artifacts are commonly observed in CTP studies and occasionally resemble myocardial perfusion defects, predominantly affecting the posterobasal wall (PB) (8). DE imaging shows promise to attenuate or even solve some technical issues related to the polychromatic nature of X-rays, driven by its ability to generate monochromatic image reconstructions.

As previously observed in other territories, within the DE group, myocardial SD levels measured at the reference segment (with normal myocardial perfusion) were highest at low energy levels, with significantly lower SD levels at increasing energy levels (17). On the opposite, myocardial SD ratio and signal-to-noise ratio were not significantly influenced by the energy level applied, possibly attributed to the fact that the energy level is inversely related both to SD and noise (17). It is noteworthy that CTP assessment of the reference segment using DE imaging at the best energy level (70 keV) showed overall similar SD levels compared to SE acquisitions.

Furthermore, it should be stressed that DE imaging was not related to an increase in radiation exposure levels compared to SE imaging.

Despite the PB segment is not commonly included in the American Heart Association classification and has therefore limited clinical implications, it serves as a consistent location of BHA. Accordingly, the ability of DE imaging to attenuate BHA at the PB segment might potentially be extrapolated to other clinically relevant left ventricular segments that are commonly affected by these artifacts such as the anterior apical wall, potentially leading to a reduction in inconclusive or false positive myocardial perfusion studies (8).

The selective filtration of low-energy photons by dense cardiac structures such as the descending aorta, the contrast-enhanced left ventricle, as well as bony structures (spine, sternum, and ribs), occasionally generates focal areas of non-physiologic hypoenhancement within the myocardium. Since all these highly attenuated structures are aligned along the same X-ray path as the PB segment, it is expected that BHA are selectively observed in these areas. Indeed, both among the DE and the SE groups, the PB segment showed significantly lower SD levels than the reference segment. Finally, we demonstrated that using DE imaging, BHA observed at low energy levels are markedly attenuated or even fade away at higher (≥70 keV) energy levels. We recognize that our findings are preliminary and hypothesis-generating, though they might potentially bear relevant clinical implications for the interpretation of CTP.

A number of limitations should be recognized. The relatively small sample size might lead to selection bias. Moreover, image acquisition requires a number of heart beats leading to potential non-uniform distribution of contrast in myocardial segments. For that reason, blood SD at both left and right ventricles was obtained and SD ratio allowed correction for potential non-uniform distribution of contrast. Finally, reproducibility analyses were not performed since we have recently shown a good interobserver agreement for the assessment of CTP using DE imaging (9).

Conclusions

DE imaging enables attenuation of BHA that influence the assessment of myocardial perfusion.

Acknowledgements

All authors have made a substantial contribution to the concept and design, acquisition of data or analysis and interpretation of data; drafted the article or revised it critically for important intellectual content; and approved the version to be published.

Disclosure: We declare that Drs. Patricia Carrascosa and Ricardo C. Cury provided consultant work for GE Healthcare in the past 12 months. There are no competing interests related to the manuscript for any of the other authors.

References

1. Meijboom WB, Van Mieghem CA, van Pelt N, et al. Comprehensive assessment of coronary artery stenoses: computed tomography coronary angiography versus conventional coronary angiography and correlation with fractional flow reserve in patients with stable angina. J Am Coll Cardiol 2008;52:636-43.
2. Meijboom WB, van Mieghem CA, Mollet NR, et al. 64-slice computed tomography coronary angiography in patients with high, intermediate, or low pretest probability of significant coronary artery disease. J Am Coll Cardiol 2007;50:1469-75.
3. Rodríguez-Granillo GA, Ingino CA, Lylyk P. Myocardial perfusion imaging and infarct characterization using multidetector cardiac computed tomography. World J Cardiol 2010;2:198-204.

4. Ko SM, Choi JW, Song MG, et al. Myocardial perfusion imaging using adenosine-induced stress dual-energy computed tomography of the heart: comparison with cardiac magnetic resonance imaging and conventional coronary angiography. Eur Radiol 2011;21:26-35.
5. Ko BS, Cameron JD, Leung M, et al. Combined CT coronary angiography and stress myocardial perfusion imaging for hemodynamically significant stenoses in patients with suspected coronary artery disease: a comparison with fractional flow reserve. JACC Cardiovasc Imaging 2012;5:1097-111.
6. Wang R, Yu W, Wang Y, et al. Incremental value of dual-energy CT to coronary CT angiography for the detection of significant coronary stenosis: comparison with quantitative coronary angiography and single photon emission computed tomography. Int J Cardiovasc Imaging 2011;27:647-56.
7. Kang DK, Schoepf UJ, Bastarrika G, et al. Dual-energy computed tomography for integrative imaging of coronary artery disease: principles and clinical applications. Semin Ultrasound CT MR 2010;31:276-91.
8. Rodríguez-Granillo GA, Rosales MA, Degrossi E, et al. Signal density of left ventricular myocardial segments and impact of beam hardening artifact: implications for myocardial perfusion assessment by multidetector CT coronary angiography. Int J Cardiovasc Imaging 2010;26:345-54.
9. Carrascosa PM, Deviggiano A, Capunay C, et al. Incremental value of myocardial perfusion over coronary angiography by spectral computed tomography in patients with intermediate to high likelihood of coronary artery disease. Eur J Radiol 2015. [Epub ahead of print].
10. George RT, Silva C, Cordeiro MA, et al. Multidetector computed tomography myocardial perfusion imaging during adenosine stress. J Am Coll Cardiol 2006;48:153-60.
11. Gibbons RJ, Balady GJ, Bricker JT, et al. ACC/AHA 2002 guideline update for exercise testing: summary article. A report of the American College of Cardiology/American Heart Association Task Force on Practice Guidelines (Committee to Update the 1997 Exercise Testing Guidelines). J Am Coll Cardiol 2002;40:1531-40.
12. Blankstein R, Shturman LD, Rogers IS, et al. Adenosine-induced stress myocardial perfusion imaging using dual-source cardiac computed tomography. J Am Coll Cardiol 2009;54:1072-84.
13. Hoffmann U, Millea R, Enzweiler C, et al. Acute myocardial infarction: contrast-enhanced multi-detector row CT in a porcine model. Radiology 2004;231:697-701.
14. Kurata A, Kawaguchi N, Kido T, et al. Qualitative and quantitative assessment of adenosine triphosphate stress whole-heart dynamic myocardial perfusion imaging using 256-slice computed tomography. PLoS One 2013;8:e83950.
15. Rossi A, Merkus D, Klotz E, et al. Stress myocardial perfusion: imaging with multidetector CT. Radiology 2014;270:25-46.
16. Schwitter J, Wacker CM, van Rossum AC, et al. MR-IMPACT: comparison of perfusion-cardiac magnetic resonance with single-photon emission computed tomography for the detection of coronary artery disease in a multicentre, multivendor, randomized trial. Eur Heart J 2008;29:480-9.
17. Carrascosa P, Capunay C, Rodriguez-Granillo GA, et al. Substantial iodine volume load reduction in CT angiography with dual-energy imaging: insights from a pilot randomized study. Int J Cardiovasc Imaging 2014;30:1613-20.

Cite this article as: Rodriguez-Granillo GA, Carrascosa P, Cipriano S, De Zan M, Deviggiano A, Capunay C, Cury RC. Beam hardening artifact reduction using dual energy computed tomography: implications for myocardial perfusion studies. Cardiovasc Diagn Ther 2015;5(1):79-85. doi: 10.3978/j.issn.2223-3652.2015.01.13

